J Mol Model (2013) 19:2273–2283
DOI 10.1007/s00894-013-1753-8

ORIGINAL PAPER

Optical properties of GaAs nanocrystals: influence of an electric field

Masoud Bezi Javan

Received: 6 November 2012 / Accepted: 2 January 2013 / Published online: 3 February 2013

Abstract A study of the electronic and optical properties of the hydrogen-terminated GaAs nanocrystals $Ga_{68}As_{68}H_{96}$ and $Ga_{92}As_{80}H_{108}$ is presented. In this study, their dielectric functions, refractive indices, and absorption coefficients were calculated using density functional theory (DFT). The influence of a uniform external electric field on the optical properties of the nanocrystals was also explored. The highest occupied molecular orbital (HOMO) and the lowest unoccupied molecular orbital (LUMO) for each nanocrystal were studied in the absence and the presence of the uniform external electric field. Our results indicate that the HOMO–LUMO gap decreases with increasing electric field strength. The calculated density of states revealed that the main reason for this shrinking gap is an increase in the delocalization of the gallium π-orbitals under the influence of an increasing external electric field. The permanent dipole moment and the polarizability of the nanocrystals under the induced electric field increased with increasing nanocrystal radius. The induced electric field caused a noticeable redshift in the absorption peaks. The electric field also increased the absorption intensity, particularly when the field strength was >0.25 V/Å.

Keywords Ab initio calculations · Nanostructures · Electronic structure · Optical properties

M. B. Javan (✉)
Department of Physics, Faculty of Sciences, Golestan University, Gorgan, Iran
e-mail: javan.masood@gmail.com

M. B. Javan
e-mail: m.javan@gu.ac.ir

Introduction

Semiconductor nanocrystals have been the focus of numerous experimental [1–3] and theoretical [4–9] studies. They also have many potential applications, such as in optoelectronic sensors [10, 11], in vivo imaging for medical diagnostics [12], quantum computing [13], solar cells [14], and nonlinear optics [15]. Recent advances in the synthesis of high-quality, 3D-confined nanocrystals have led to a detailed understanding of the sensitivity of the dependence of their physical properties on nanocrystal size [16].

So far, considerable attention has been directed toward the preparation of GaAs nanostructures [17–24]. GaAs, one of the most important group III–V semiconductors, is suitable for use in high-efficiency solar cells because it has a band gap that is near-ideal (1.43 eV) for single-junction solar cells [25]. Furthermore, it exhibits high optical absorption, meaning that a GaAs solar cell only needs to be a few microns thick to absorb sunlight. GaAs is also preferred for use in the space industry due to its insensitivity to heat and its high resistance to radiation damage. GaAs nanoparticles with dimensions on the order of only a few nanometers have been prepared by various techniques, including laser ablation, molecular beam epitaxy, radiofrequency (rf) sputtering, and chemical methods [26–30].

The application of an external electric field in order to tune the energy gap of a semiconductor nanocrystal can be an important step in the development of electronic and optoelectronic devices. The effects of electric fields on the electronic and optical properties of semiconductor nanostructures have been intensively investigated over the last few years [31–35]. The presence of local electric fields can lead to changes in the absorption spectrum due to the Stark effect.

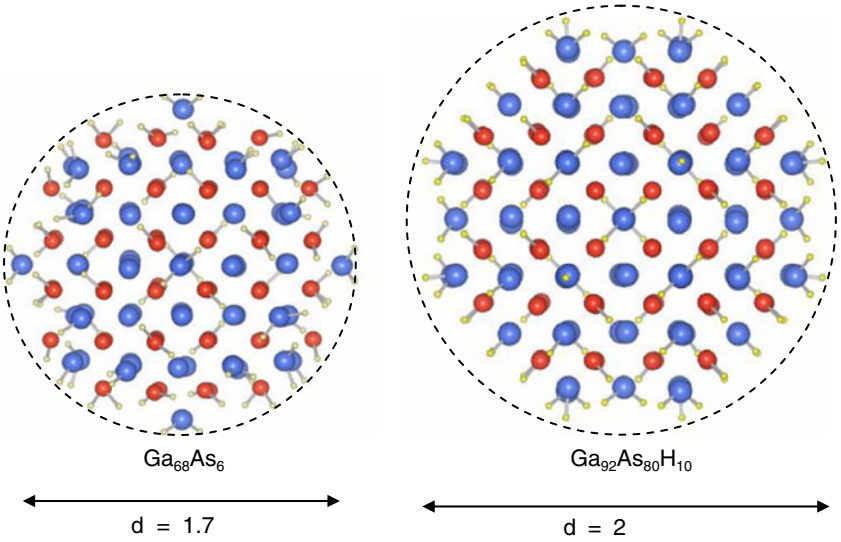

Fig. 1 The optimized geometries of the $Ga_{68}As_{68}H_{96}$ and $Ga_{92}As_{80}H_{108}$ nanocrystals. Parameter *d* is the diameter of the nanoparticle

While experimental studies can be used to characterize material properties precisely, theoretical investigations can be employed to estimate the general behavior of a material in a vast range of applications. Recently, we have studied the electronic and optical properties of small GaAs nanoparticles (with diameters of 6–15 Å) [36]. By applying an appropriate generalized gradient approximation (GGA) in density functional theory (DFT), a survey of larger nanoparticles could highlight some important properties. In the work described in the present paper, we calculated the electronic and optical properties of $Ga_{68}As_{68}H_{96}$ and $Ga_{92}As_{80}H_{108}$ nanocrystals as well as the influence of an external electric field on their energy gaps and optical absorption properties. This paper is organized as follows: in "Simulation methods," we briefly describe the theoretical framework we used in our study, while the "Results and discussion" and "Conclusions" sections discuss, respectively, the results obtained in our study concerning the electronic and optical properties of the nanocrystals, and the conclusions that can be drawn from them.

Simulation methods

Computational details

We studied spherical GaAs nanocrystals with diameters of 1.7 nm ($Ga_{68}As_{68}H_{96}$) and 2 nm ($Ga_{92}As_{80}H_{108}$) using the linear combination of atomic orbitals (LCAO) technique and pseudopotential density functional calculations. The GaAs nanocrystals were modeled by considering all of the bulk

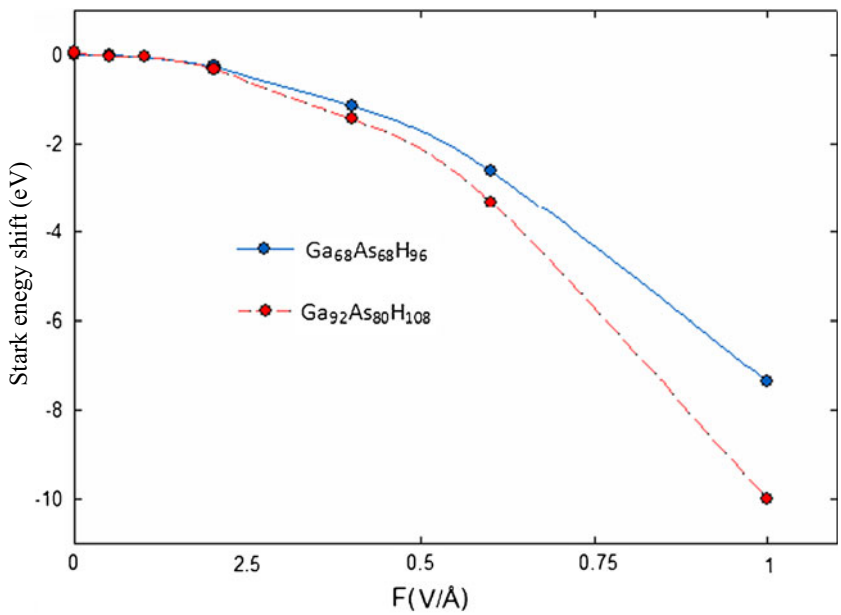

Fig. 2 Stark energy shifts of the two GaAs nanocrystals versus electric field strength

Table 1 Permanent dipole moments of the two nanocrystals considered here and polarizabilities in the direction of the electric field

Nanocrystal	μ_0 (eÅ)	α (eÅ^2/V)
$Ga_{68}As_{68}H_{96}$	1.285	39.792
$Ga_{92}As_{80}H_{108}$	1.423	49.645

GaAs atoms present within a sphere of a given radius and by terminating surface dangling bonds with hydrogen atoms. For each nanocrystal, calculations were performed in both the absence and the presence of a uniform external electric field. The structural properties were determined by allowing all of the atoms of each GaAs nanocrystal to relax fully. It is worth pointing out that the starting GaAs nanocrystals had T_d symmetry. The GaAs nanocrystals were placed in a large cubic supercells with dimension of 20 Å from each x, y and z direction in order to remove the additional interactions with similar structures in a periodic lattice. A careful convergence analysis of both the electronic and the structural properties was performed with respect to the LCAO basis set cutoff. Full geometry optimization was implemented by carrying out ab initio calculations based on the generalized gradient approximation (GGA) with the Perdew–Burke–Ernzerhof (PBE) functional [37] in density functional theory (DFT) and standard norm-conserving Troullier–Martins pseudopotentials [38]. The total energy of the molecular system and the Hellmann–Feynman forces acting on the atoms were calculated with convergence tolerances of 10^{-4}eV and 0.02 eV/Å, respectively. In the present work, we extended the optical response calculations to take into account the effects of nanocrystal size and a uniform external electric field. We used the results of our calculations with the optimal basis set to compute the dielectric functions of the GaAs nanocrystals.

Table 2 HOMO and LUMO energy levels (eV) and HOMO–LUMO gaps (E_g) of the nanocrystals in the presence of various electric fields (V/Å)

Nanocrystal	F (V/Å)	HOMO	LUMO	E_g
$Ga_{68}As_{68}H_{96}$	0	−2.01	0.411	2.421
	0.05	−1.66	0.742	2.402
	0.15	−1.566	0.782	2.348
	0.25	−1.344	0.843	2.187
	0.35	−0.851	0.893	1.744
	0.6	−0.616	0.482	1.098
	1	−0.08	0.086	0.167
$Ga_{92}As_{80}H_{108}$	0	−1.019	0.811	1.830
	0.05	−0.946	0.879	1.825
	0.15	−0.842	0.894	1.736
	0.25	−0.748	0.75	1.498
	0.35	−0.453	0.452	0.905
	0.6	−0.143	0.339	0.482
	1	−0.052	0.01	0.062

Theoretical description

It is well known that the electric field of incoming light can polarize materials according to the following relation [39]:

$$P^i(\omega) = \chi^{(1)}_{ij}(-\omega, \omega) \cdot E^j(\omega), \quad (1)$$

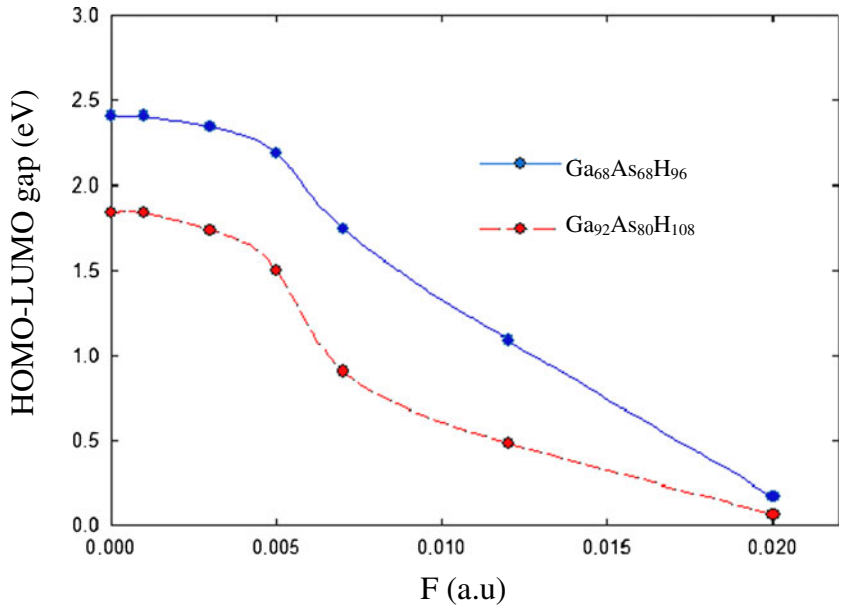

Fig. 3 Variations in the HOMO–LUMO gaps (eV) of the GaAs nanocrystals versus electric field strength

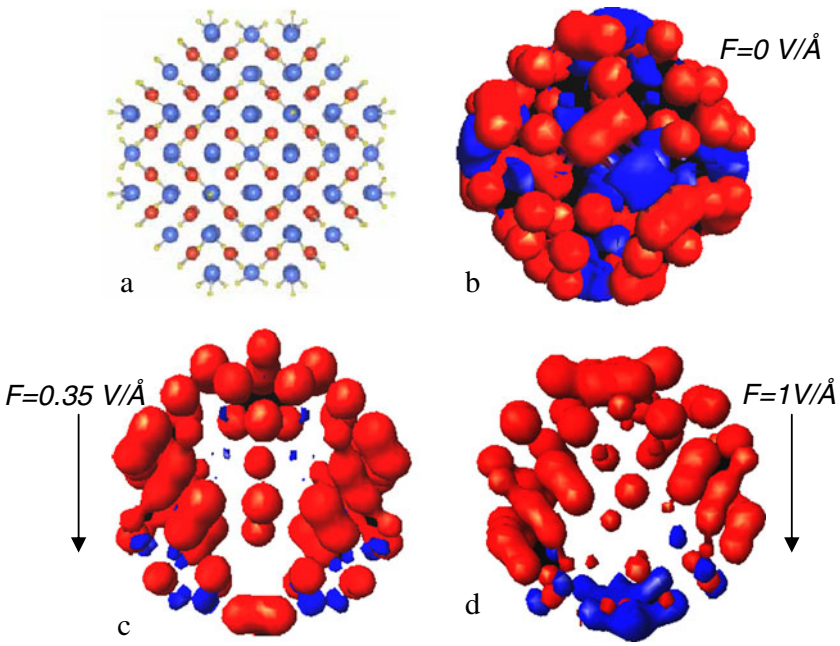

Fig. 4a–d Optimized geometry of the $Ga_{92}As_{80}H_{108}$ nanocrystal (**a**), and electron charge density difference in this nanocrystal at **b** F=0, **c** F=0.35 and **d** F=1 V/Å

where $\chi_{ij}^{(1)}$ is the linear optical susceptibility tensor, given by [40]

$$\chi_{ij}^{(1)}(-\omega,\omega) = \frac{e^2}{h\Omega}\sum_{nm\,\vec{k}} f_{nm}\left(\vec{k}\right)\frac{r_{nm}^{i}\left(\vec{k}\right)r_{mn}^{i}\left(\vec{k}\right)}{\omega_{mn}\left(\vec{k}\right)-\omega} = \frac{\varepsilon_{ij}(\omega)-\delta_{ij}}{4\pi}. \tag{2}$$

In the above relation, n and m indicate energy bands, $\vec{k}$ is the reciprocal lattice vector, $f_{mn}\left(\vec{k}\right) \equiv f_m\left(\vec{k}\right) - f_n\left(\vec{k}\right)$ is the Fermi occupation factor, Ω is the normalized volume, and $\omega_{mn}\left(\vec{k}\right) \equiv \omega_m\left(\vec{k}\right) - \omega\left(\vec{k}\right)$ is the frequency difference. $\vec{r}_{mn}$ is a matrix element of the position operator, and is given by

$$r_{nm}^{i}\left(\vec{k}\right) = \begin{cases} \frac{v_{nm}^{i}(k)}{i\omega_{nm}}; & \omega_n \neq \omega_m \\ 0 & \omega_n = \omega_m \end{cases}, \tag{3}$$

where $v_{nm}^{i}\left(\vec{k}\right) = \mu^{-1}p_{nm}^{i}\left(\vec{k}\right)$, μ is the free electron mass, and $\vec{p}_{nm}$ is a momentum matrix element. According to the above relations, the dielectric function is defined as:

$$\varepsilon_{ij}(\omega) = 1 + 4\pi\chi_{ij}^{(1)}(-\omega,\omega). \tag{4}$$

The imaginary part (ε_2) of the dielectric function can be obtained from

$$\varepsilon_2^{ij}(\omega) = \frac{e^2}{h\pi}\sum_{nm}\int d\vec{k}\, f_{nm}\left(\vec{k}\right)\frac{v_{nm}^{i}\left(\vec{k}\right)v_{nm}^{j}\left(\vec{k}\right)}{\omega_{mn}^{2}} \delta\left(\omega-\omega_{mn}\left(\vec{k}\right)\right). \tag{5}$$

Using the Kramers–Kronig transformation, the real part of the dielectric function can be expressed as

$$\varepsilon_1^{ij}(\omega) = \frac{2}{\pi}P\int_0^{\infty}\frac{\omega'\varepsilon_2^{ij}(\omega')}{\omega' 2-\omega^2}d\omega'. \tag{6}$$

The optical response of the hydrogen-terminated GaAs nanocrystals was evaluated in SIESTA [41]. The calculated optical matrix elements included corrections for the nonlocality of the pesudopotential [42]. The refractive index, N, and the optical absorption coefficients of the nanocrystals then can be calculated by the following formula [43]:

$$N = \sqrt{\frac{\sqrt{\varepsilon_1^2(\omega)+\varepsilon_2^2(\omega)}+\varepsilon_1(\omega)}{2}} \tag{7}$$

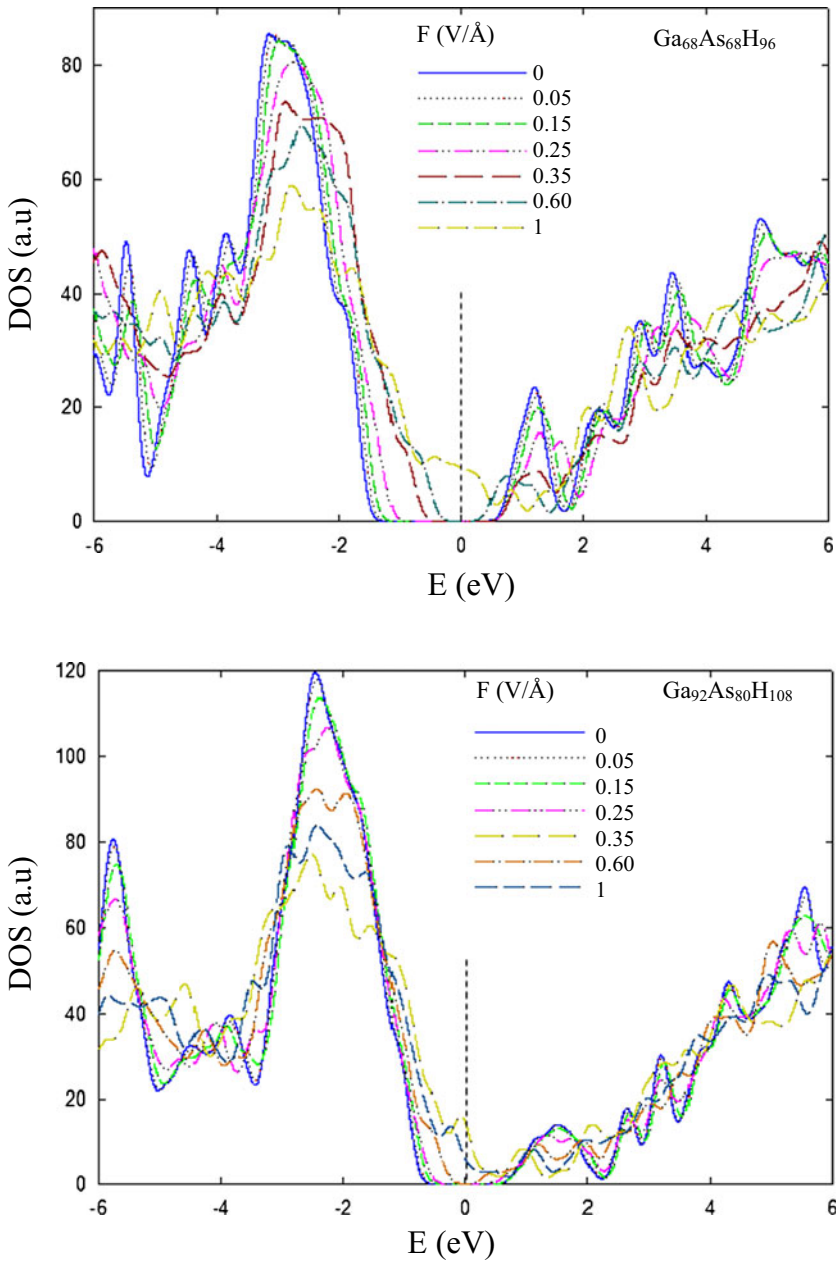

Fig. 5 The electronic density of states (DOS) of each nanocrystal in the absence and the presence of an electric field

$$\alpha = 2\frac{\omega}{c}\sqrt{\frac{\sqrt{\varepsilon_1^2(\omega)+\varepsilon_2^2(\omega)}-\varepsilon_1(\omega)}{2}}. \quad (8)$$

Results and discussion

Figure 1 shows the atomic configurations of the studied GaAs nanocrystals. The GaAs nanocrystals have zincblende lattice structures terminated by hydrogen atoms. The optimized geometric structures were obtained at the GGA-PBE level of theory with a numerical atomic orbital basis, as implemented in the SIESTA code [41]. We used the double-zeta polarized basis set (DZP) for both atomic species, and each configuration was relaxed until the forces fell below 0.02 eV/Å. The diameters of the $Ga_{68}As_{68}H_{96}$ and $Ga_{92}As_{80}H_{108}$ nanocrystals were 1.7 and 2 nm, respectively. In the GGA-PBE calculations performed on our nanocrystals, the central Ga–As bond lengths were near to 2.46 Å, which is close to the bulk Ga–As bond length (2.44 Å). For all of the atomic bonds near the nanocrystal surface, we saw a relative increase in the bond length in comparison to that in the bulk state: the average Ga–As bond length was 2.56 Å. The mean Ga–H and As–H bond lengths in the two cases studied were 1.55 and 1.53 Å, respectively. Also, the symmetry of the nanocrystals changed from T_d to the C_1 point group upon atomic force minimization.

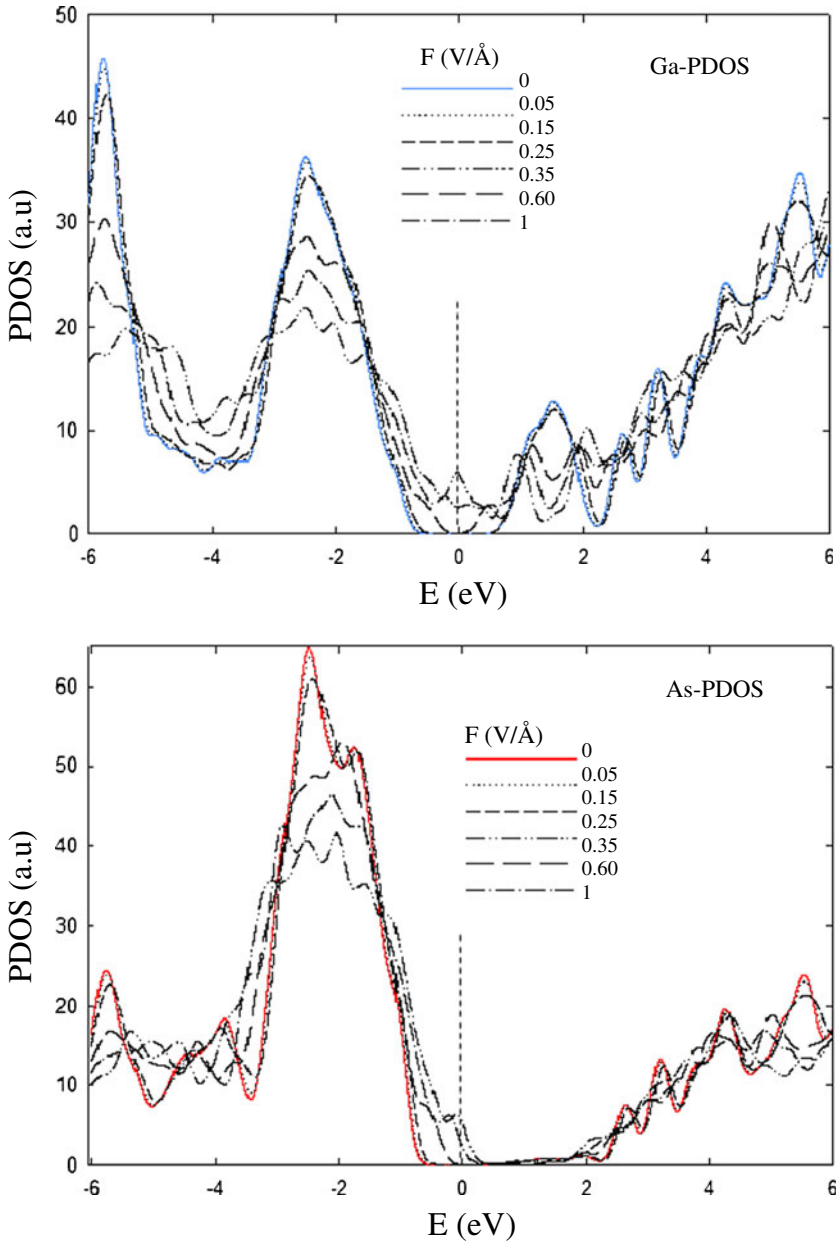

Fig. 6 The projected electronic density of states (PDOS) on the As atoms and the PDOS on the Ga atoms of a $Ga_{92}As_{80}H_{108}$ nanocrystal in the absence and the presence of an electric field

In this work, we explored the effect of an electric field on the electronic and optical properties of GaAs nanocrystals. To observe whether a local electric field can broaden and redshift the maxima of absorption peaks, electric fields of different strengths (ranging from 0.05 to 1 V/Å) were applied to the nanocrystals. When a dc electric field is applied to a semiconductor, a change in the optical absorption spectrum may result; this is termed "electroabsorption" [44]. Increasing the intensity of absorption peaks, peaks broadening and redshift in the optical absorption can be the main role of the applied electric field in optoelectronic devices. Changing the strength of the external applied electric field influences the interactions between electronic states of the nanoparticles due to the Stark effect. It is therefore interesting to look at the Stark shift of the nanocrystals in an electric field. Figure 2 shows the dependence of the Stark shift of the equilibrium state on the electric field strength. The energy shift is calculated as $\Delta E(R) = E(F,R) - E(F=0, R)$, and is a function of both the nanoparticle radius (R) and the applied electric field (F). The Stark shifts of the nanocrystals increase as the electric field strength increases. It is well known that the energy shift of one nanocrystal has a linear dependence on the applied field in the presence of a permanent dipole moment, while a quadratic dependence can arise due to the quantum-confined Stark effect (QCSE) [45]. The relation between the Stark shift and the dipole moment can

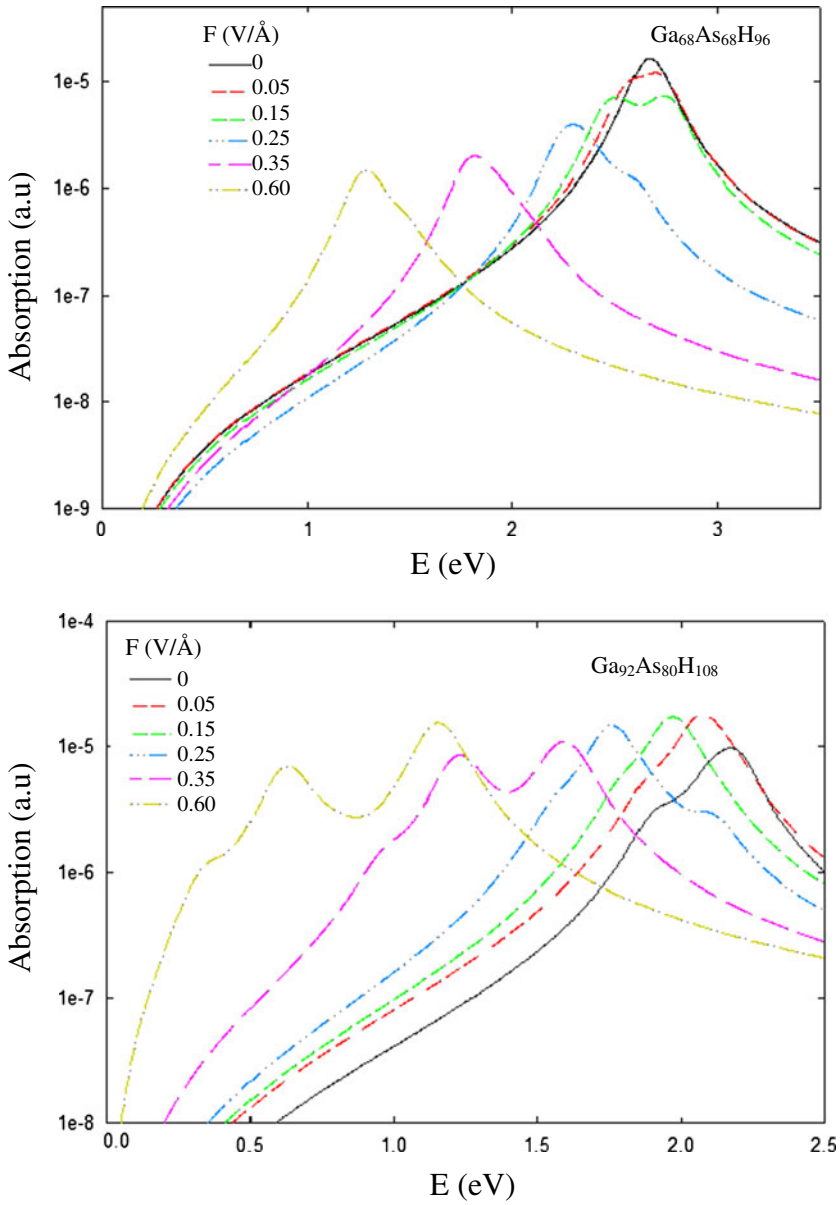

Fig. 7 Absorption coefficients of the two GaAs nanocrystals exposed to various electric field strengths

be estimated using the following equation:

$$-\Delta E(F) = \mu_0 F + \frac{\alpha}{2} F^2, \tag{4}$$

where μ_0 and α are the permanent dipole and the polarizability in the direction of the electric field, respectively. The permanent dipole moments of the two nanocrystals considered here and their average polarizabilities in the direction of the electric field are shown in Table 1.

The localizations and energies of the molecular orbitals (MOs) reveal the characteristics of the excited states and provide insight into the absorption spectra of the nanocrystals. Regarding their electronic properties, the presence of a uniform external electric field decreases the energy gap between the highest occupied single particle state (HOMO) and the lowest unoccupied single-particle state (LUMO). Figure 3 shows the variation in the HOMO–LUMO gap for each nanocrystal versus electric field strength. The HOMO–LUMO gaps of the $Ga_{68}As_{68}H_{96}$ and $Ga_{92}As_{80}H_{108}$ nanocrystals are 2.421 and 1.830 eV, respectively. The HOMO–LUMO gaps of the nanocrystals gradually decrease when an external electric field is applied; note that the rate of decrease reduces when the electric field strength drops below 0.25 V/Å. At electric field strengths of >0.25 V/Å, the HOMO–LUMO gaps of the nanocrystals vary significantly. In Table 2, the HOMOs, LUMOs, and HOMO–LUMO gaps of the nanocrystals in the presence of various electric fields are listed. In the presence of an electric field, delocalization of the HOMO and LUMO increases and the tails of the HOMO and LUMO

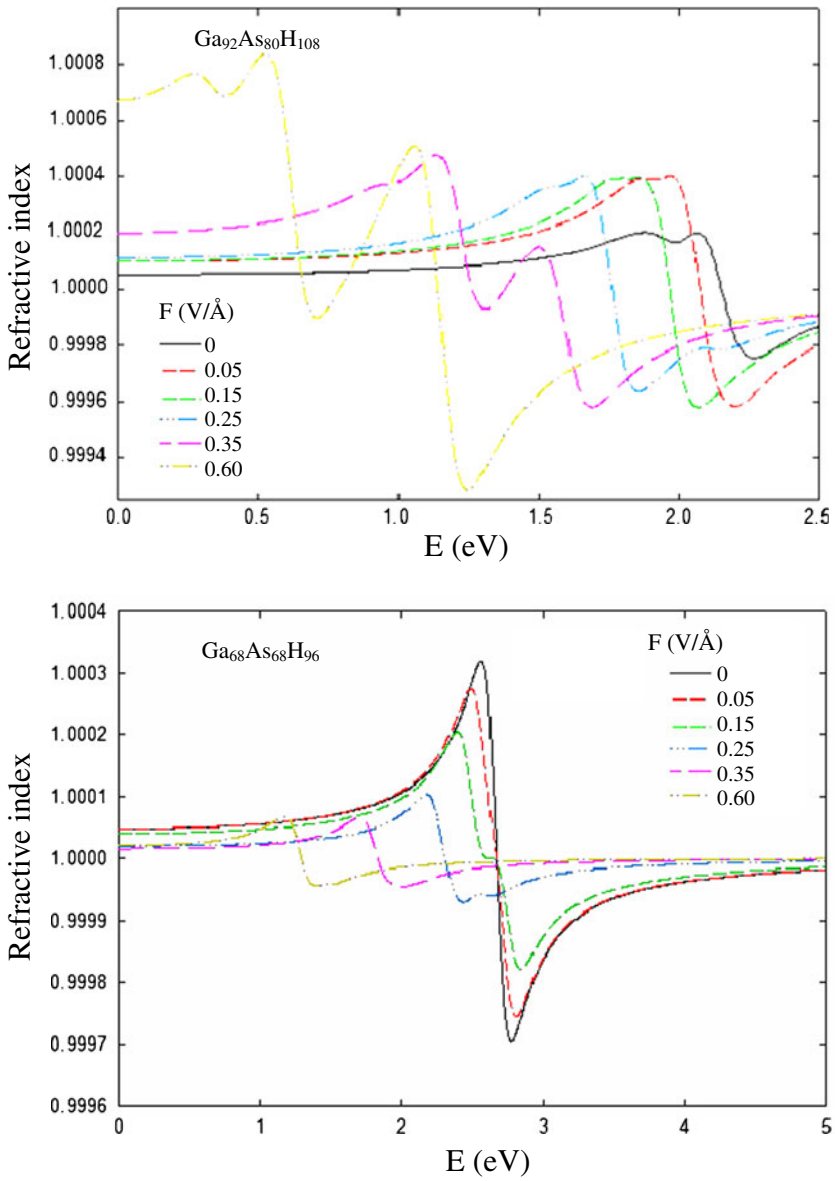

Fig. 8 Energy dispersion of the refractive index for each GaAs nanocrystal exposed to various electric fields

wavefunctions elongate in the gap region. There is a critical electric field strength near to 0.25 V/Å at which a significant change occurs in the HOMO and LUMO energy levels of the nanocrystals. To investigate this phenomenon further, Fig. 4 shows the electron charge density difference of a $Ga_{92}As_{80}H_{108}$ nanocrystal versus field strength. The blue and red parts in the figure indicate the decrease and increase of the charge density. It is clear from the figure that the presence of a uniform external electric field can change the symmetry of the electronic charge density in comparison with nanocrystals without an electric field present. Looking at the red and blue regions, we can conclude that charge concentrations arise due to the increase in the field strength in the direction opposite to the electric field at the positions of atoms in the nanocrystal.

Density of states analysis is able to accurately describe the electronic state behavior of nanocrystals in the presence of an electric field. In Fig. 5, we plot the density of states of each nanocrystal in the absence and presence of an electric field. In order to compare the electronic and the hole states of the nanocrystals in the presence of an electric field, we show the density of states of each nanocrystal at different field strengths (from 0.05 to 1 V/Å). Degenerate electron levels are destroyed with the application of the electric field, and new energy levels are shifted into the gap region. The electronic states shift toward more positive energies while hole states shift to more negative energies. To investigate this further, the projected density of states (PDOS) on the Ga atoms and the PDOS on the As atoms in the $Ga_{92}As_{80}H_{108}$ nanocrystal were plotted, as shown in Fig. 6. As can be seen,

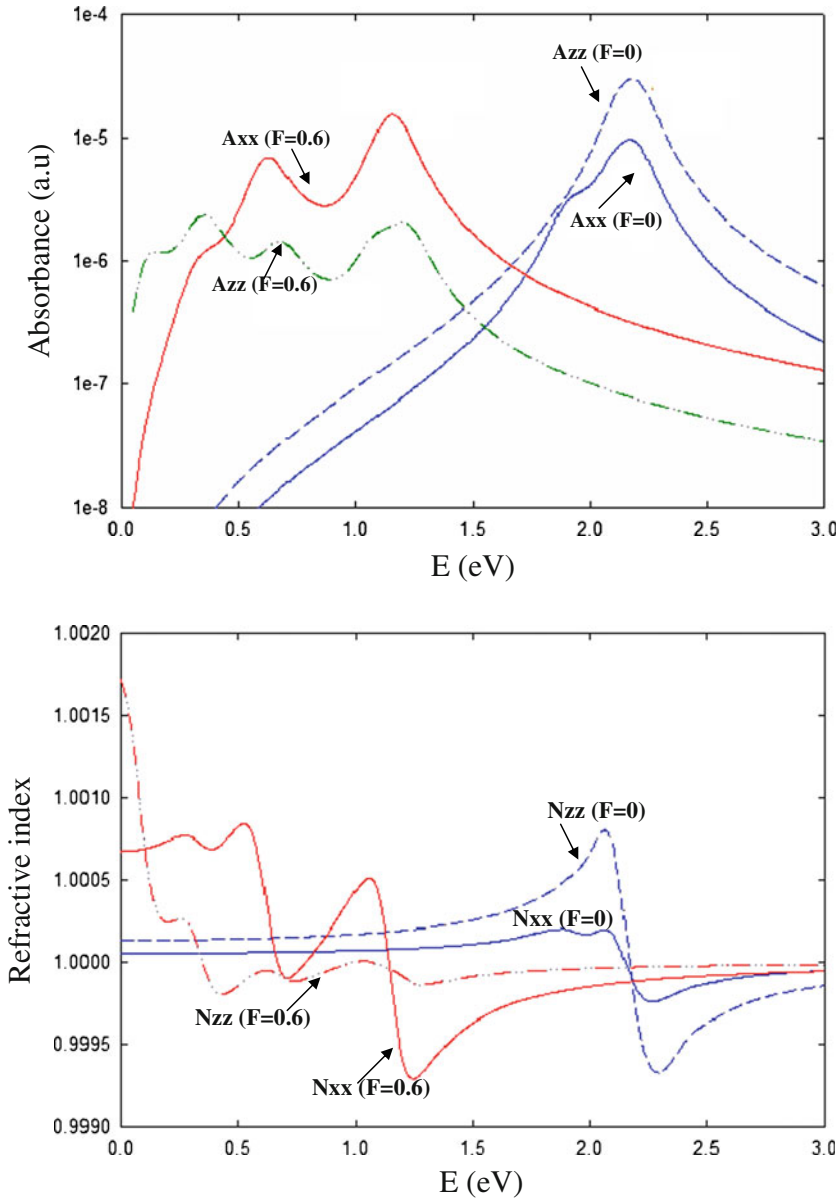

Fig. 9 Dependences of the anisotropic behavior of the absorption and the refractive index of a $Ga_{92}As_{80}H_{108}$ nanocrystal on the electric field strength (V/Å)

increasing the field strength significantly broadens the electronic states distributed from −2 to −4 eV. Considering the PDOSs on the Ga and As atoms, it is easy to conclude that the gallium π-electronic states are more delocalized than the arsenic π-electronic states are, thus indicating that gallium π-orbital delocalization is the main reason for the decrease in the energy gap in the presence of an electric field.

The origin of the optical properties is the interaction of a photon with the electrons. This interaction can fully described in terms of the transitions between occupied and unoccupied states due to the interaction of electric field of the incident light with the electronic steady states of the system. When the transitions are independent, they are known as single-particle excitations, and the spectra resulting from these excitations can be thought of as a joint density of states between the valence and conduction bands, weighted by appropriate matrix elements to introduce selection rules. In Fig. 7, we show the absorption coefficients of the considered GaAs nanocrystals. In the case of the $Ga_{68}As_{68}H_{96}$ nanocrystal, the absorption is concentrated in the 2.2–3.4 eV region, while the active region for the $Ga_{92}As_{80}H_{108}$ nanocrystal is 1.5–2.8 eV. The induced electric field cause noticeable redshifts in the absorption peaks due to changes in the electronic structures of the nanocrystals and thus the transition probabilities between occupied and unoccupied states. On the other hand, the presence of the electric field decreases the absorption intensity, particularly at field strengths of more than 0.1 V/Å. Figure 8 shows the energy dispersion of the refractive index for each GaAs nanocrystal in various electric fields. As shown in the figure,

$Ga_{68}As_{68}H_{96}$ exhibits a sharp refractive index peak at 2.55 eV. The induced electric field shifts this peak towards the lower-energy region while significantly reducing the value of the refractive index. In the case of the $Ga_{92}As_{80}H_{108}$ nanocrystal, the refractive index peak occurs at 2.12 eV. The electric field shifts this peak towards the lower-energy region, and the value of the refractive index increases as the electric field strength rises.

To investigate further, the dependencies of the absorption coefficient and the refractive index of each nanocrystal on the direction of incidence of the photons were studied, which arise due to the anisotropy of the dielectric function. In Fig. 9, the absorption coefficient and refractive index of the $Ga_{92}As_{80}H_{108}$ nanocrystal for two components (*xx* and *zz*) of the dielectric function are presented. The external electric field is applied in the *x* direction. In Fig. 9, we also present the influence of the electric field on the absorption and the refractive index anisotropy of the $Ga_{92}As_{80}H_{108}$ nanocrystal. It is noticeable that the *yy* component of the dielectric function is the same as the *zz* component ($\varepsilon_{xx} = \varepsilon_{yy}$). As is clear from the figure, at zero electric field, the *zz* components of the absorption coefficient and refractive index peaks are stronger than those for the *xx* components of these peaks. In the presence of the electric field, in addition to the redshifts of the adsorption and refractive index peaks, the absorption and the refractive index increase in the direction of the electric field. The reverse situation occurs in the direction perpendicular to the field. The *zz* components of the absorption coefficient and refractive index peaks decrease significantly with increasing electric field, although the presence of the electric field causes new peaks to arise in the interval 0–0.5 eV for the $Ga_{92}As_{80}H_{108}$ nanocrystal.

Conclusions

In this study, we theoretically probed the electronic and optical properties of two hydrogen-terminated gallium arsenide nanocrystals with average diameters of 1.7 and 2 nm, respectively, using density functional theory. We also investigated the influence of an induced external electric field on the electronic and optical properties of these GaAs nanocrystals. Our investigation of the electronic charge densities of the nanocrystals showed that the electric field can disturb the symmetry of the charge density. The energy shift in the electronic structures of the nanocrystals that occurs upon the application of a uniform external electric field (Stark effect) was studied. Our results show that the Stark shift increases with rising electric field strength. We also found that the Stark shifts at fields of ~0.5 V/Å are sensitive to nanocrystal size, as the larger nanocrystal showed a greater Stark shift. The permanent dipole moment and polarizability of the nanocrystals in an induced electric field increase with nanocrystal radius. The highest occupied molecular orbital (HOMO) and the lowest unoccupied molecular orbital (LUMO) for each nanocrystal were studied in the absence and the presence of a uniform external electric field. Our results indicate that the HOMO–LUMO gap decreases with increasing electric field strength. The calculated density of states reveals that the main reason for this gap reduction is the increase in the delocalization of the gallium π-orbitals with a rising external electric field. The gallium π-orbitals, which occupy electronic states near the edge of the gap, are separated upon applying a uniform external electric field, leading to new states in the gap region. The optical absorption and refractive index of each nanocrystal were also investigated. The energy gap reduction that occurs upon applying a uniform external electric field leads to a redshift in the optical absorption of each nanocrystal. The same behavior can also be seen for the refractive indices of the nanocrystals. In addition, we found that these GaAs nanocrystals exhibit significant absorption anisotropy, and that their optical properties are sensitive to the direction of incidence of the photons and the induced external electric field strength.

Acknowledgments This work was supported by a grant (no. 91001105) from the Iran National Science Foundation (INSF).

References

1. O'Brien SC, Liu Y, Zhang Q, Heath JR, Tittel FK, Curl RF, Smalley RE (1986) Supersonic cluster beams of III–V semiconductors: Ga_xAs_y. J Chem Phys 84:4074–4080
2. Zhang QL, Liu Y, Curl RF, Tittel FK, Smalley RE (1987) Photodissociation of semiconductor positive cluster ions. J Chem Phys 88:1670–1678
3. Schafer R, Becker JA (1996) Photoabsorption spectroscopy on isolated Ga_NAs_M clusters. Phys Rev B 54:10296–10299
4. Graves RM, Scuseria GE (1991) Ab initio theoretical study of small GaAs clusters. J Chem Phys 95:6602–6607
5. Liao DW, Balasubramanian K (1992) Electronic structure of the III–V tetramer clusters and their positive ions. J Chem Phys 96:8938–8948
6. Andreoni W (1992) III-V semiconductor microclusters: structures, stability, and melting. Phys Rev B 45:4203–4207
7. Yi JY (2000) Atomic and electronic structures of small GaAs clusters. Chem Phys Lett 325:269–274
8. Zhao W, Cao PL, Li BX, Song B (2000) Study of the stable structures of Ga_4As_4 cluster using FP-LMTO MD method. Phys Rev B 62:17138–17143
9. Zhao W, Cao PL (2001) Study of the stable structures of Ga_6As_6 cluster using FP-LMTO MD method. Phys Lett A 288:53–57
10. Chen W, Zhang JZ, Joly AG (2004) Optical properties and potential applications of doped semiconductor nanoparticles. J Nanosci Nanotech 4:919–947
11. Costa-Fernandez JM, Pereiro R, Sanz-Medel A (2006) The use of luminescent quantum dots for optical sensing. Trends Anal Chem 25:207–218
12. Michalet X, Pinaud FF, Bentolila LA, Tsay JM, Doose S, Li JJ, Sundaresan G, Wu AM, Gambhir SS, Weiss S (2005) Quantum

dots for live cells, in vivo imaging and diagnostics. Science 307:538–544
13. Calarco T, Datta A, Fedichev P, Pazy E, Zoller P (2003) Spin-based all-optical quantum computation with quantum dots: understanding and suppressing decoherence. Phys Rev A 68:012310–012331
14. Schaller RD, Klimov VI (2006) Non-Poissonian exciton populations in semiconductor nanocrystals via carrier multiplication. Phys Rev Lett 96:097402–097406
15. Karamanis P, Begue D, Pouchan C (2007) Ab initio finite field (hyper)polarizability computations on stoichiometric gallium arsenide clusters Ga_nAs_n ($n = 2-9$). J Chem Phys 127:094706–094716
16. Murray CB, Norris DJ, Bawendi MG (1993) Ab initio finite field (hyper) polarizability computations on stoichiometric gallium arsenide clusters Ga_nAs_n ($n = 2-9$). J Am Chem Soc 115:8706–8715
17. Masumoto Y, Matsuura M, Tarucha S, Okamoto H (1985) Direct experimental observation of two-dimensional shrinkage of the exciton wave function in quantum wells. Phys Rev B 32:4275–4278
18. Olshavsky MA, Goldstein AN, Alivisatos AP (1990) Organometallic synthesis of gallium-arsenide crystallites, exhibiting quantum confinement. J Am Chem Soc 112:9438–9439
19. Butler L, Redmond G, Fitzmaurice D (1993) Preparation and spectroscopic characterization of highly confined nanocrystallites of gallium arsenide in decane. J Phys Chem 97:10750–10755
20. Sun Y, Rogers JA (2004) Fabricating semiconductor nano/microwires and transfer printing ordered arrays of them onto plastic substrates. Nano Lett 4:1953–1959
21. Berry AD, Tonucci RJ, Fatemi M (1996) Fabrication of GaAs and InAs wires in nanochannel glass. Appl Phys Lett 69:2846–2849
22. Duan X, Wang JL, Lieber CM (2000) Synthesis and optical properties of gallium arsenide nanowires. Appl Phys Lett 76:1116–1119
23. Duan X, Lieber CM (2000) General synthesis of compound semiconductor nanowires. Adv Mater 12:298–302
24. Shi W, Zheng Y, Wang N, Lee CS, Lee ST (2001) A general synthetic route to III–V compound semiconductor nanowires. Adv Mater 13:591–594
25. Streetman BG, Sanjay B (2000) Solid state electronic devices, 5th edn. Prentice Hall, Upper Saddle River
26. Fu Y, Willander M, Sivchenko EL (2000) Photonic dispersions of semiconductor-quantum-dot-array-based photonic crystals in primitive and face-centered cubic lattices. Superlatt Microstruct 27:255–264
27. Hirasawa M, Ichikawa N, Egashira Y, Honma I, Komiyama H (1995) Synthesis of GaAs nanoparticles by digital radio frequency sputtering. Appl Phys Lett 67:3483–3486
28. Perriere J, Millon E, Chammaro M, Morcrette M, Andreazza C (2001) Formation of GaAs nanocrystals by laser ablation. Appl Phys Lett 78:2949–2951
29. Malik MA, Brien PO, Norager S, Smith J (2003) Gallium arsenide nanoparticles: synthesis and characterisation. J Mater Chem 13:2591–2595
30. Ganeev RA, Ryasnyanskiy AI, Usmanov T (2007) Optical and nonlinear optical characteristics of the Ge and GaAs nanoparticle suspensions prepared by laser ablation. Opt Commun 272:242–246
31. Tews M, Pfannkuche D (2002) Stark effect in colloidal indium arsenide nanocrystal quantum dots: consequences for wave-function mapping experiments. Phys Rev B 65:073307–073311
32. Sheng W, Leburton JP (2002) Anomalous quantum-confined Stark effects in stacked InAs/GaAs self-assembled quantum dots. Phys Rev Lett 88:167401–167405
33. Sheng W, Leburton JP (2001) Enhanced intraband transitions with strong electric-field asymmetry in stacked InAs/GaAs self-assembled quantum dots. Phys Rev B 64:153302–153306
34. Zhang P, Zhao XG (2001) Localization and entanglement of two interacting electrons in a double quantum dot. J Phys Condens Matter 13:8389–8393
35. Chang K, Xia JB (1998) The effects of electric field on the electronic structure of a semiconductor quantum dot. J Appl Phys 84:1454–1460
36. Bezi Javan M (2012) First principles study of the electronic and optical properties of GaAs nanoparticles under the influence of external uniform electric field. Phys Lett A 376:3241–3247
37. Perdew JP, Burke S, Ernzerhof M (1999) Generalized gradient approximation made simple. Phys Rev Lett 77:3865–3868
38. Troullier N, Martins JL (1991) Efficient pseudopotentials for plane-wave calculations. Phys Rev B 43:1993–2006
39. Levine ZH, Allan DC (1989) Linear optical response in silicon and germanium including self-energy effects. Phys Rev Lett 63:1719–1722
40. Philipp H, Ehrenreich RH (1963) Optical properties of semiconductors. Phys Rev 129:1550–1560
41. Soler JM, Artacho E, Gale JD, Garcia A, Junquera J, Or-dejon P, Portal SD (2002) The SIESTA method for ab initio order-*N* materials simulation. J Phys Condens Matter 14:2745–2749
42. Read AJ, Needs RJ (1991) Calculation of optical matrix elements with nonlocal pseudopotentials. Phys Rev B 44:13071–13073
43. Griffiths DJ (1999) Introduction to electrodynamics. Prentice Hall, Upper Saddle River
44. Butcher P, Cotter D (1990) The elements of nonlinear optics. Cambridge University Press, Cambridge
45. Empedocles SA, Bawendi MG (1997) Quantum-confined Stark effect in single CdSe nanocrystallite quantum dots. Science 278:2114–2117